



Pharmacophore-based Screening of Antimycobacterial 2-Pyrone-Tethered Nitrobenzothiazinone

Mary P. Kagoro^{1*} • Samuel Atte² • Lokta Solomon¹

¹ Department of Chemistry, University of Jos, Plateau State, Nigeria

² Department of Integrated science educations, Adamu Tafawa Balewa College of Education, Kangere, Bauchi State Nigeria
kagoromary@yahoo.com

Abstract. Rational and structure-based drug design is more efficient than the traditional method of drug discovery because this method examines the molecular basis of disease and uses the three-dimensional structure of the biological target. A series of 2-pyrone derivatives of Nitrobenzothiazinone were developed and evaluated for their drug-likeness, solubilities and pharmacokinetic and pharmacodynamic data employing two free software packages (SwissADME and admetSAR). The compounds were further evaluated for their binding affinities against DprE1, an essential enzyme involved in fatty acid biosynthesis, leading to cell death of *Mycobacterium tuberculosis* (*M. tuberculosis*) and three of compounds showed affinities higher than 5-nitrobenzothiazinone. Virtual screening showed a high molecular similarity (<90%) between the developed ligands. The potential of 2-pyrone-tethered Nitrobenzothiazinone towards DprE1 indicates the need for further evaluation in animal studies against both *M. tuberculosis* and other non-tuberculous Mycobacteria.

To cite this article

[Kagoro, M. P., Atte, S. Solomon, L. (2019). Pharmacophore-based Screening of Antimycobacterial 2-Pyrone-Tethered Nitrobenzothiazinone. *The Journal of Middle East and North Africa Sciences*, 5(10), 1-10]. (P-ISSN 2412- 9763) - (e-ISSN 2412-8937). www.jomenas.org. **1**

Keywords: 2-pyrone-tethered Nitrobenzothiazinone, Virtual Screening, DprE1, Molecular Dynamics (MD), Pharmacophore Mapping, Drug Design, Anti-Tubercular Agents.

1. Introduction:

Developing new drugs is challenging, costly, and is flawed with low success rates. The vast majority of drugs evaluated in clinical trials do not reach the market due to high attrition rate (Lahti *et. al.*, 2012). Drug development is a balance between optimizing druglike properties, efficacy, safety, and pharmacokinetic data. Therefore, the early stage of drug discovery focuses on identifying molecules that can bind to a target. Though potency is a driving factor in these early stages, the pharmacokinetic and toxicity properties are better indicators of drug success than potency. The pharmacokinetic profile of a compound defines its absorption, distribution, metabolism, and excretion (ADME) properties. Optimal binding properties of a new drug to its cellular target are vital, but drug concentration at its target site that produces the desired physiological effect in the clinic is more relevant. Hence, the recent attention on virtual screening of the ADME properties which has led to a significant reduction in the number of compounds that fail in clinical trials due to poor ADME properties (Hoang *et al.*, 2017; Yang *et al.*, 2018).

There are several strategies such as Lipinski's "Rule of 5" (Lipinski *et al.*, 1997; Lipinski, 2016), and Egan Egg (Egan *et al.*, 2000; Egan & Lauri, 2002), as guidelines that constitute a filter on what drug might be

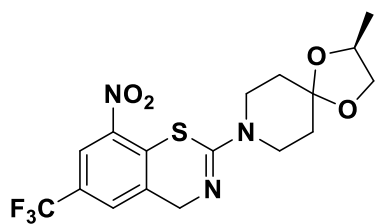
well- or poorly absorbed, and which are brain permeant, and which are non-permeant. The strategies try to identify broad chemical properties that may increase a molecule's chances to reach the market, within a large and unexplored chemical space (Reymond and Awale, 2012). Another is data mining which seeks to explore the extensive data available within pharmaceutical companies and the internet, (Qing *et al.*, 2014) though there are still challenges within these filters. But the early ADME profiling of drug candidates is now a crucial component in the success of any new compound and has been integrated into the drug development process which should hopefully mitigate late-stage drug failure. More so, evaluation of experimental ADMET properties is time-consuming and costly. Hence the use of virtual or *in silico* screening to optimize pharmacokinetics and toxicity properties to obtain leads that progress to drug candidates. There are many *in silico* approaches for predicting pharmacokinetics and toxicity properties of compounds from their chemical structure (Mascarenhas & Gottlieb, 1975), ranging from data mining approaches such as quantitative structure-activity relationship (Kaloga & Christiansen, 1981), similarity searches (Kuroyanagi *et al.*, 1982), and three-dimensional QSAR (Shin *et al.*, 2016), to structure-based methods such as ligand-protein docking (Sagawa *et al.*, 2005) and



pharmacophore mapping which is based on ligand properties (Giddens et al., 2008). Some of these *in silico* methods are freely available but several are not thus limiting the application of these methods in drug design and development.

Tuberculosis (TB) is an infection caused by *Mycobacterium tuberculosis* that affects the lung, and all other major organs and tissues of the body. At least 2.3 billion people worldwide are infected with this bacterium. The control of TB has led to increase in the prevalence of multi-resistant (MDR) and extensively drug-resistant (XDR) TB. The challenges with current TB drugs, is the long period of drug regimen, raising cases of resistant TB including the recent report of totally resistant TB (TR-TB) and the coinfection of TB and HIV. To address these challenges, efforts have been directed towards TB drug design and development. Traditional methods of antibiotic discovery have failed to keep pace with the evolution of this resistance. Over the last few years, progress has been made in the search for new anti-TB compounds (De Luca et al., 2009). However, strains resistant to these new molecules have already been reported (Parretti et al., 1997; Boucher et al., 2009; Arias and Murray 2008). The search for new drugs against TB plays a crucial role in meeting sustainable development goals (SDG) and in achieving global worldwide goals established by the WHO (WHO 2016; De Lima and Nascimento, 2013). Infections caused by resistant bacteria are harder to treat and are associated with increasing healthcare costs in addition to higher mortality (Cleves et al., 2006). There is a need for novel treatment strategies to combat these resistant bacteria. Moreover, the high attrition rate of drug design research draws on the need for a more collaborative and holistic approach to drug discovery and development.

In 2009, Makarov *et al.*, (2009), described Nitrobenzothiazinone (BTZ043; Figure 1) as a new class of compounds with high anti-mycobacterial activity.



BTZ043

Figure 1. Nitrobenzothiazinone an anti-tuberculosis drug undergoing clinical trials.

DprE1 is a decaprenyl phosphoryl-D-ribose oxidase, involved in the biosynthesis of decaprenyl phosphoryl-D-arabinose (DPA), an essential component of the mycobacterial cell wall and is essential for cell

growth and survival (Hann et al., 2001). The most promising BTZ compound BTZ043 (Fig 1) is characterized by a nitro group, opined to be fundamental to the anti-TB activity. The high 'drug ability' of DprE1 is proven by the numerous structurally unrelated compounds that inhibit this enzyme. BTZ043 is the most promising inhibitor of DprE1 studied in recent times and we chose it as our target of interest because of this drug ability and tethered 2-pyrone compounds to BTZ043 to further evaluate the effect that these modifications would have on the drug-likeness, physicochemical and binding affinities of the designed compounds and DprE1 (Figure 2; DprE1 docking simulation with the designed compounds).

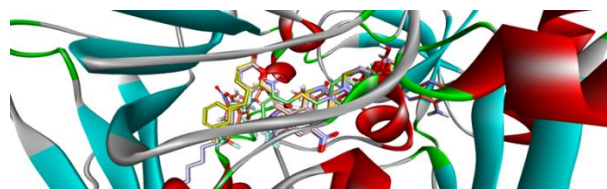


Figure 2. Docking pose of 2-pyrone-tethered 5-nitrobenzothiazinone.

2-Pyrone motif is ubiquitous in nature and a wide range of activities have been reported for them such as cytotoxicity against HeLa cells (Fang et al., 2015) anticancer against human breast cancer (Fairlamb et al., 2004), antimicrobial activity (Fairlamb et al., 2004), protein kinase C inhibition (Zhao et al., 2015), and inhibition of cyclic AMP-dependent protein kinase (Peltola et al., 2001). Nocapyrones A-J (Figure 3) below are reported to have neuroprotective activities in inflammation-related brain damage induced by microglial cell activation (Yamashita et al., 1988; Dolak et al., 1980). Severe brain inflammation could lead to neuronal cell death and is believed to be a cause of Parkinson's disease, Alzheimer's disease or cerebral ischemia (Stoll et al., 1998; Kim & Joh, 2006). In this same vine, Myxopyronin A, B and coralopyronin A, B and Csypyrone Bs (B1-B3) are novel inhibitors of RNA polymerase (RNAP) that binds this protein in a different manner to other known antibiotics (Kreutzberg, 1996). In line with our interest in designing 2-pyrone-based anti-TB drugs, we are exploring the combination of Nitrobenzothiazinone with 6-styryl-2-pyrone and screening them for their drug-likeness, synthetic accessibility, their ADMET profile and their physicochemical properties relative to Nitrobenzothiazinone.

Pharmacophore mapping involves computer-based methods that recognises ligands' molecular features essential for biological activity. It is employed to reduce the number of compounds to purchase, test and synthesise in any drug design and discovery research.

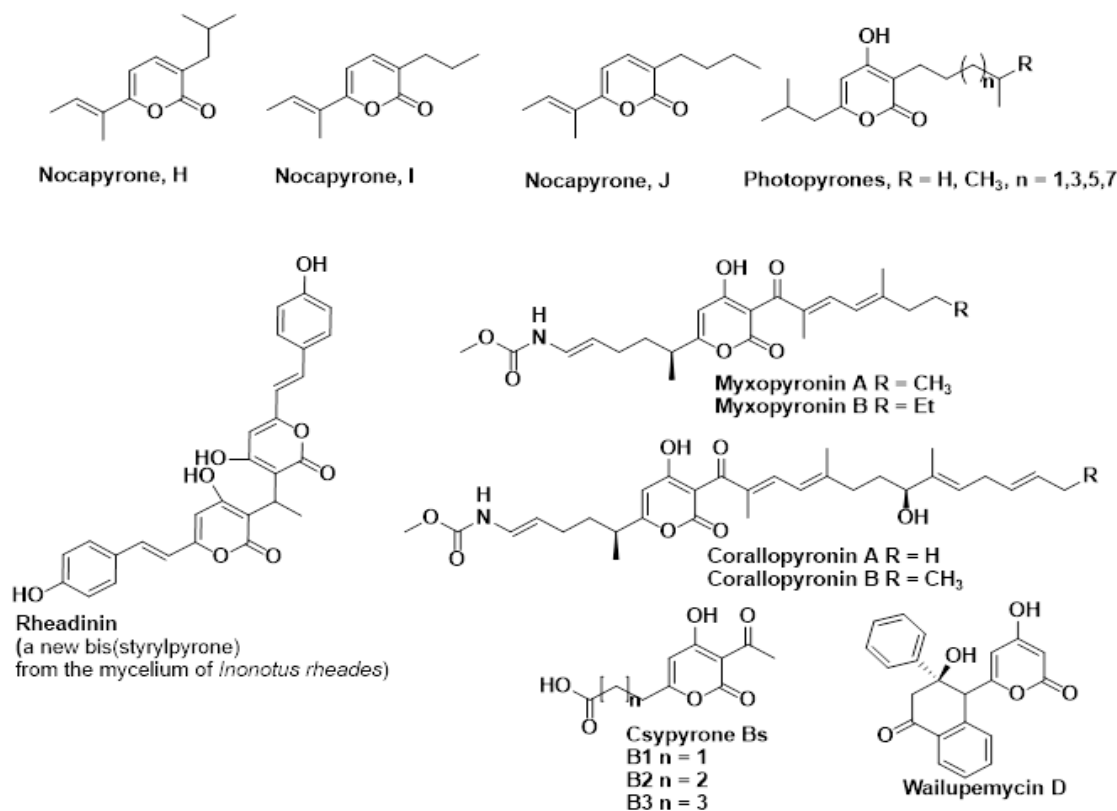


Figure 3: Selected Natural and Biologically active 2-pyrone Compounds.

It leads to a reduction in cost of rational/modern drug discovery relative to conventional drug design process (Tsai et al., 2008; Day et al., 2009). It involves three steps: identifying elements responsible for biological activity, generating the different poses the ligands can adopt and determine the 3D relationship between each element in the generated poses. Herein, we employ pharmacophore mapping to design 2-pyrone-based anti-TB drug-like compounds in line with our interest in developing anti-tuberculosis drugs (figure 4).

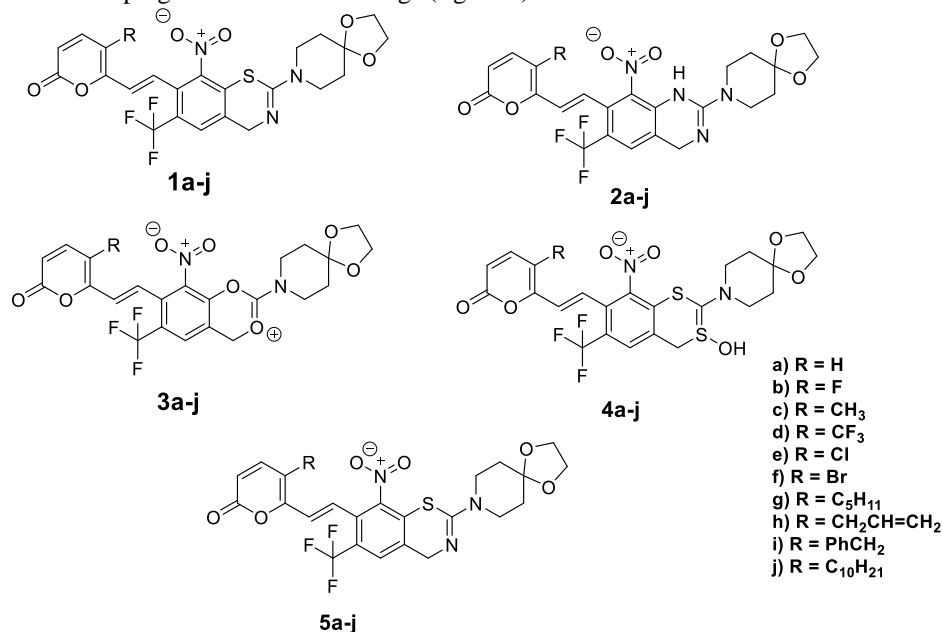


Figure 4. 2-Pyrone-tethered 5-nitro-benzothiazinone.



2. Methodology:

A designed dataset of a fifty 2-pyrone-tethered 5-nitrobenzothiazinone compounds containing alkyl, aryl and halide groups as structural key elements were used to perform 3D-QSAR studies. In such investigations, the molecular alignment and conformation determination are very important for the reliability and validity of the resulting model. The availability of X-ray data from crystallized protein-ligand complexes enabled the inclusion of additional information from the receptor site. Therefore, we applied a strategy of combining conformations obtained by employing bio isosteric (H and F, CH₃ and CF₃, Cl, and Br) for pharmacophoric alignment. In this case, we mapped the 2-pyrone scaffold onto 5-nitrobenzothiazinone to obtain structural molecules with high similarity (<95%) to each other and moderate similarity to (BTZ043, similarity score ca 50%) as showed in figure 5 below.

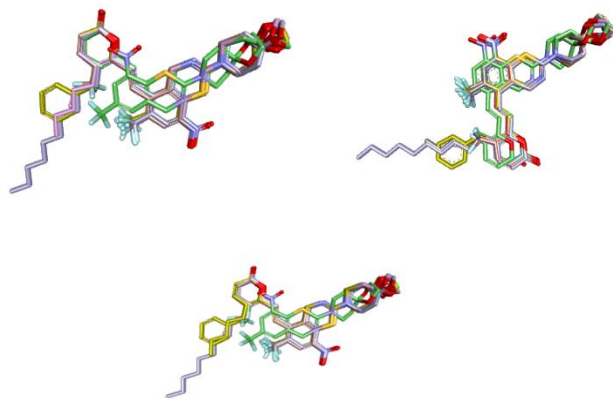


Figure 5: Molecular alignment of the designed compounds to BTZ043.

2.1. Preparation for Virtual Screening: The designed dataset containing 50 compounds were drawn using ChemDraw 16. The Protein Drug Bank (PDB) structure of DprE1 protein (PDB Code: 6hf0, Makarov et al., 2014), was retrieved from the PDB (<http://www.rcsb.org/pdb/home/home.do>).

2.2. First Round of Screening Based on Lipinski's and Egan's Lead-Likeness Criteria: The 50 compounds were filtered to exclude compounds that did not follow SwissADME lead-likeness criteria (Daina et al., 2017), ($150 < MW < 500$, $-3.5 < C \log P < 4.5$, $0 < \text{number of rings} < 5$, $0 < \text{rotational bonds} < 10$, $0 < \text{donors} < 5$, $0 < \text{acceptors} < 10$ (Daina et al., 2017; Lipinski et al., 1997). The filtered compounds contained 45 potential lead compounds (Fig 4). Based on the results in Table 1, we screened out molecules with more than three filters (or limits) as indicated by the red-colored highlights. Therefore, twenty compounds were dropped leaving us with 30 molecules to advance to the next stage. Some of the parameters that were calculated included iLOGP which is the closest to atom-based LogP 98 (ALogP98), and ADME 2D Topological Polar Surface Area (TPSA).

2.3. ADMET Prediction: To estimate the drug-likeness of the compounds, *in silico* absorption, distribution, metabolism, excretion, and toxicity (ADMET) prediction was carried out (Lagorce et al., 2011). We investigated the ADMET properties of the 10 selected compounds using the ADMET Protocol in the SwissADME software package (Christ et al., 2010). These studies were solely based on the chemical structure of the molecule. Some of the parameters that were calculated include the Blood-Brain Barrier (BBB), Cytochrome P4502D6 (CYP2D6), Cytochrome P4501A19 (CYP1A19), Cytochrome P4503A4 (CYP3A4), Cytochrome P4502C9 (CYP2C9) and Cytochrome P4501A1 (CYP1A1). The designed

Table 1: Physicochemical properties for designed compounds 1a-j.

Entry	1a	1b	1c	1d	1e	1f	1g	1h	1i	1j
Mol. wt.	523.48	541.47	537.51	591.5	602.38	557.93	593.61	563.35	613.6	663.75
#Heavy atoms	36	37	37	40	37	37	41	39	43	46
#arom. Heavy atoms	12	12	12	12	12	12	12	12	18	12
fraction Csp3	0.39	0.39	0.41	0.42	0.39	0.39	0.5	0.38	0.33	0.58
#rot. Bonds	5	5	5	6	5	5	9	7	7	14
# H-B acceptors	10	11	10	10	13	10	10	10	10	10
#H-B donors	0	0	0	0	0	0	0	0	0	0
MR	134.2	134.15	139.16	139.2	141.9	139.21	158.39	148.3	163.65	182.43
TPSA	135.39	135.39	135.39	135.4	135.39	135.39	135.39	135.39	135.39	135.39
logP o/w (ILOGP)	3.6	3.7	3.63	3.78	3.78	3.67	4.5	4.01	4.08	5.66
LogS (ESOL)	-5.31	-5.31	-5.34	-5.92	-6.06	-5.74	-6.70	-6.74	-5.81	-8.49

compounds were found to be non-inhibitors of CYP1A2 and CYP2C19. Whilst compounds **1g** and **1j** are inhibitors of CYP2D6 in addition, all the compounds were druglike with the exception of **1f**, **1i** and **1j** (Table 2) employing Lipinski's filter guideline.

activity. We further attempted to optimize the structures and focused on two aspects: (a) introduction of a series of chemical bridges (-NH-, -O- or -S-) to eliminate planarity and enhance drug-likeness. (b) Different substitutions introduced to C-6 and C-8 positions of the Nitrobenzothiazinone ring to improve potency was taken

Table 2: Results of the pharmacokinetics, drug likeness and lead likeness.

ENTRY	1a	1b	1c	1d	1e	1f	1g	1h	1i	1j
GI absorption	low	low	low	low	low	low	low	low	low	low
BBB permeant	No	No	No	No	No	No	No	No	No	No
P-gp Substrate	Yes	Yes	Yes	Yes	Yes	Yes	Yes	No	Yes	Yes
CYP1A2 inhibitor	No	No	No	No	No	No	No	No	No	No
CYP2C19 inhibitor	No	No	No	No	No	No	No	No	No	No
CYP2C9 inhibitor	Yes	Yes	Yes	Yes	Yes	Yes	Yes	Yes	Yes	No
CYP2D6 inhibitor	No	No	No	No	No	No	Yes	No	No	Yes
CYP3A4 inhibitor	No	No	No	No	No	No	Yes	No	No	No
DRUGLIKENESS	Yes	Yes	Yes	Yes	Yes	Yes	No	Yes	No	No
LEADLIKENESS	No	No	No	No	No	No	No	No	No	No

2.4. Second Round of Screening: Based on Docking PyRx virtual screening package was used to screen 45 compounds in the database by docking (Autogrid, 2019). For the docking studies, the X-ray crystallographic structure of the DprE1 complexed with BTZ043 (PDB Code: 6hf0) from the Protein Data Bank (PDB) was used. The PDB protein and converted to pdbqt format by PyRx and Openbabel (O'Boyle et al., 2011). A grid box with dimensions of 25×25×25 Å (-4.0157, -12.402, 18.7581) with a spacing of 0.313 Å² was constructed around the docking area using PyRx software (Autogrid, 2019). Molecules were docked using Vina with exhaustiveness grade of 8, with up to nine poses saved per molecule. The docking procedure was carried out for the unchanged conformation of the receptor and flexible ligand molecules. BTZ043 was redocked in the 6hf0 model to validate the docking algorithms of PyRx docking program (the root-mean-square deviation value is 2.254). The lowest energy conformations were selected and the ligand interactions with DprE1 were determined.

3. Results and Discussion:

conjugates of Nitrobenzothiazinone and 6-styryl-2-pyrone fight against different diseases but modular molecules against anti-tuberculosis are urgently needed. Synthetic methods for substituted 2-pyrone and Nitrobenzothiazinone derivatives have been reported (Lipinski et al., 1997; Makarov et al., 2014; Daina et al., 2017), however, so far, their combined activities have not been investigated. From data mining it was reported that Nitrobenzothiazinone (**figure 5**) showed significant anti-tuberculosis activity against Mtb with MIC values of 0.004 μM and 5-substituted 6-styryl-2-pyrone showed significant activity against Mtb, this inspired us to conduct the structure-based and ligand-based activity combining both for more potent anti-tuberculosis

into account but the change in substitution pattern did not lead to a significant change in ADMET nor solubility score for these compounds. Moreover, it should be mentioned that in order to evaluate the contribution of Nitrobenzothiazinone and 2-pyrone to the anti-tuberculosis activity, respectively, the replacements of Nitrobenzothiazinone with naphthalene and 2-pyrone with a phenyl ring were conducted and their binding affinity were also evaluated.

The pharmacokinetic profile of all the molecules under investigation was predicted by ADMET models provided by the SwissADME program. The human intestinal absorption (HIA) and the blood-brain barrier (BBB) models. Polar surface area (PSA) has an inverse relationship with percent HIA, and thus with cell wall permeability (Palm et al., 1997). Although a relationship between PSA and permeability has been demonstrated, the models usually do not consider the effects of other descriptors. Despite the general use of logP to estimate a compound's lipophilicity, logP is a ratio (Arnott & Planey, 2012). Thus, the hydrogen bonding characteristics obtained by calculating the PSA could be considered along with the logP calculation (Pliska et al., 1996). According to the model, a compound with optimum cell permeability should follow the criteria PSA < 140 Å² and ILOGP < 5 (Pliska et al., 1996). All the compounds showed PSA < 140 Å², and all compounds showed PSA < 140 Å², and all compounds, except **1J** had ILOGP < 5 (**Table 1**).

The solubility of the designed compounds varied from poorly soluble to insoluble (**Table 1**). Cytochrome P450 2D6 (CYP2D6) metabolises numerous compounds and its inhibition has the potential for dangerous drug-drug interactions (DDIs, Gonzalez and Gelboin 1992). Determination of CYP2D6 inhibition is therefore important in drug discovery and it is the only Cytochrome P450 that is non-inducible as others are

made more active by the presence of some drugs (e.g. rifampicin induces CYP2C9). All the designed compounds were non-inhibitors of CYP2D6, except **1h** and **1i**. In addition, all but **1h** are non-inhibitors of CYP3A4. All the compounds were classified as inhibitors of CYP2C9 except **1j** (Table 2). CYP2C9 is fundamental to the metabolism of 25% of drugs in common use in the clinic (e.g. tamoxifen, diclofenac, and ibuprofen). Drug interactions arise when one of the inhibitor drugs is administered with drugs with a low therapeutic index such as S-warfarin and phenytoin. Azole antifungal drugs work by inhibition of the fungal cytochrome P450 14 α -demethylase. This interrupts the conversion of lanosterol to ergosterol, a component of the fungal cell membrane. The possible use of fungal P450s, as a target against human pathogenic fungi is generating a lot of interest. (Trott & Olson, 2010).

The pharmaceutical activity is determined by the free drug concentration; therefore, the possible plasma protein binding of compounds must be considered (Moroy et al., 2012). Six of the 30 tested compounds were likely to be <90% binding, five were likely to be \geq 90% binding, and 19 were likely to be \geq 95% binding (Table 3). Plasma protein binding refers to the degree to which medications attach to proteins within the blood. A drug's efficiency may be affected by the degree to which it binds. The less bound a drug is, the more efficiently it can traverse cell membranes or diffuse.

Table 3: Binding affinity in Kcal/mol of 6hf0 with BT043

Binding affinity / Kcal/mol	mode	RMSD Lower	RMSD UPPER
-13.3	0	0	0
-13.2	1	5.425	7.606
-13.1	2	3.627	6.831
-13.1	3	2.759	6.144
-13	4	3.095	4.273
-12.9	5	2.64	3.393
-12.8	6	18.637	19.828
-12.8	7	1.649	4.817
-12.7	8	12.396	14.354

Due to the ADMET predictions, the docking studies, and chemical structures (refers to structural modification) compounds **1a-c**, **2a-c** and **3a-c** are suitable for further *in vitro* and *in vivo* evaluation. In the docking study, the developed compounds formed hydrogen bond interactions with N of the **Gly 109** and **Ala 104** to fluorine of the trifluoromethyl group on the middle-fused phenyl group. There are several unfavorable interactions with groups of Ile 83, Pro316, Ala 104, and Ala 105.

The middle-fused phenyl ring of 5-nitrobenzothiazinone hydrophobic interactions with the

corresponding parts of **Phe 108**, **Ala 104**, **Ala 105**, **Pro 107**, **Met 102** and **Lys 149**. Halogen interaction between **Ala 105**, **Phe 108** and **Pro 107**. Thus, the developed compounds could be used as potential hits for further *in vitro* and *in vivo* evaluation.

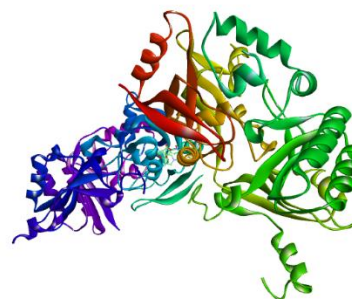


Figure 6. Picture showing the docking pose of 1c in 6hf0.

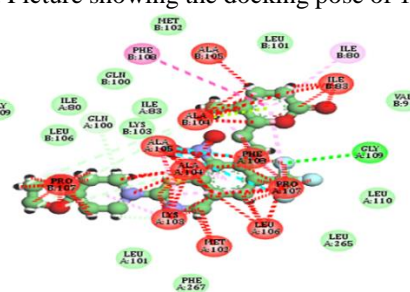


Figure 7. Picture showing the various interactions between 1c and 6hf0.

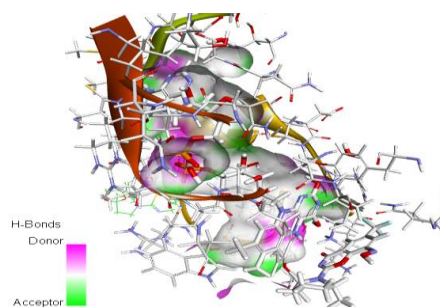


Figure 8: Picture showing protein interaction around the ligand surface as solved by Bio solve software package.

3.1. Molecular Docking: Structure-based drug design is a tool for reducing the overall period for drug discovery. As precise knowledge of protein-ligand complexes can lead to the design and optimization of new compounds with better intermolecular interactions and/or improvement of the physicochemical profile of the lead compound without perturbing the interaction between the drug and the target. X-ray crystallography and NMR spectroscopy are the two most relevant techniques for obtaining protein-ligand complexes. One limitation with X-ray crystallography is the requirement of crystallizing the complex and this is still an issue even with the



advancement in the area (DeLucas, 2001). High-resolution structure determination using NMR spectroscopy has many disadvantages, but the major disadvantage is the need to observe, resolve and sign numerous protein signals though this can be solved by employing labeling procedures such as per deuteration (Opella et al., 2001).

In the absence of high-resolution structural data on protein-ligand complexes, computational docking strategies can be used to attempt prediction of not only the ligand-binding site (Liang et al., 1998), but also the structure of the protein-ligand complex for use in structure-based design (Kuntz et al., 1994; Hajduk et al., 2004). This research reports the binding affinity of 2-pyrone tethered 5-nitrobenzothiazinone compounds with DprE1. Employing the first screening filter as stated above we would have screened compounds **1h**, **1i** and **1j**. Evaluation of the compounds anyway led to potential drug compounds that were better binder than the antitubercular compound **BTZ043** (Tables 4-8).

Table 4: Binding affinity in Kcal/mol of **6hf0** with **1b**.

Binding affinity / Kcal/mol	mode	RMSD Lower	RMSD UPPER
-13.5	0	0	0
-13.2	1	2.908	7.063
-13.2	2	3.816	7.958
-13.1	3	4.524	8.424
-13.1	4	6.094	10.104
-13	5	3.522	5.746
-12.9	6	10.75	12.938
-12.8	7	1.532	5.915
-12.8	8	4.998	7.569

Table 5: Binding affinity in Kcal/mol of **6hf0** with **1c**

Binding affinity / Kcal/mol	mode	RMSD Lower	RMSD UPPER
-13.8	0	0	
-13.7	1	4.211	8.383
-13.6	2	2.61	6.908
-13.5	3	3.762	7.847
-13.5	4	5.009	8.826
-13.4	5	3.7	5.998
-13.3	6	6.254	10.317
-13.3	7	4.157	5.349
-13.2	8	6.551	9.754

Table 6: Binding affinity in Kcal/mol of **6hf0** with **1i**

Binding affinity / Kcal/mol	mode	RMSD Lower	RMSD UPPER
-15.4	0	0	0
-15	1	3.021	7.733

-14.7	2	3.166	6.781
-14.6	3	3.67	5.448
-14.5	4	4.667	6.502
-14.5	5	5.829	9.482
-14.4	6	6.694	9.513
-14.3	7	6.748	10.86
-14.2	8	3.71	4.967

Table 7: Binding affinity in Kcal/mol of **1h** with **6hf0**.

Binding affinity / Kcal/mol	mode	RMSD Lower	RMSD UPPER
-15.5	0	0	0
-15.3	1	3.236	6.391
-15.2	2	12.904	16.216
-15.1	3	2.308	5.976
-15	4	5.096	7.007
-15	5	3.361	6.94
-14.9	6	4.689	9.088
-14.9	7	12.988	16.208
-14.8	8	13.425	16.523

Table 8: Binding affinity in Kcal/mol of **1j** with **6hf0**.

Binding affinity / Kcal/mol	mode	RMSD Lower	RMSD UPPER
-15.4	0	0	0
-15.3	1	1.482	5.386
-15.1	2	11.584	15.201
-15	3	12.217	15.466
-15	4	11.22	4.02
-14.9	5	3.555	6.523
-14.8	6	10.064	13.562
-14.7	7	2.324	3.292
-14.6	8	17.716	19.4

The binding affinity shows that compounds **1b**, and **1c** had binding affinity values similar to that of the antitubercular compound **BTZ043** as showed in Tables 4-6 whilst compounds **1h**, **1i** and **1j** had higher binding affinities as showed in Tables 7-9. The implication of this is that we have successfully designed molecules that are better binder to this Mtb target enzyme. More so, the experimental values of these compounds should be evaluated for the possible new anti-tuberculosis drug candidate. The other compounds showed similar trend amongst their type hence we can use the results below to represent the whole set.

Acknowledgments: The authors wish to appreciate the head of the Department of Chemistry, University of Jos, Nigeria. My Ph.D. Supervisors (Professors Simon Duckett and Ian Fairlamb, of the Department of Chemistry, University of York, United Kingdom) for their support and criticism that awakened my



consciousness to drug design and in silico-based drug design, I will be forever grateful.

Corresponding Author:

Mary P. Kagoro, Ph.D.

Department of Chemistry, University of Jos, Plateau State, Nigeria

E-mail : kagoromary@yahoo.com

References:

- Arias, C. A., & Murray, B. E. (2008). Emergence and management of drug-resistant enterococcal infections. *Expert review of anti-infective therapy*, 6(5), 637-655.
- Arnott, J. A., & Planey, S. L. (2012). The influence of lipophilicity in drug discovery and design. *Expert opinion on drug discovery*, 7(10), 863-875.
- Autogrid. (2019). Accessed on 26 February 2018. Available online: <http://autodock.scripps.edu/wiki/AutoGrid>
- Boucher, H. W., Talbot, G. H., Bradley, J. S., Edwards, J. E., Gilbert, D., Rice, L. B., ... & Bartlett, J. (2009). Bad bugs, no drugs: no ESKAPE! An update from the Infectious Diseases Society of America. *Clinical infectious diseases*, 48(1), 1-12.
- Cleves, A. E., & Jain, A. N. (2006). Robust ligand-based modeling of the biological targets of known drugs. *Journal of medicinal chemistry*, 49(10), 2921-2938.
- Christ, F., Voet, A., Marchand, A., Nicolet, S., Desimmié, B. A., Marchand, D., ... & De Maeyer, M. (2010). Rational design of small-molecule inhibitors of the LEDGF/p75-integrase interaction and HIV replication. *Nature chemical biology*, 6(6), 442.
- Daina, A., Michielin, O., & Zoete, V. (2017). SwissADME: a free web tool to evaluate pharmacokinetics, drug-likeness and medicinal chemistry friendliness of small molecules. *Scientific reports*, 7, 42717.
- Day, P. J., Cleasby, A., Tickle, I. J., O'Reilly, M., Coyle, J. E., Holding, F. P., ... & Jhoti, H. (2009). Crystal structure of human CDK4 in complex with a D-type cyclin. *Proceedings of the National Academy of Sciences*, 106(11), 4166-4170.
- De Lima, L. A. C. V., & Nascimento, A. S. (2013). MolShaCS: a free and open source tool for ligand similarity identification based on Gaussian descriptors. *European journal of medicinal chemistry*, 59, 296-303.
- De Luca, L., Barreca, M. L., Ferro, S., Christ, F., Iraci, N., Gitto, R., ... & Chimirri, A. (2009). Pharmacophore-based discovery of small-molecule inhibitors of protein-protein interactions between HIV-1 integrase and cellular cofactor LEDGF/p75. *ChemMedChem*, 4(8), 1311-1316.
- DeLucas, L. J. (2001). Protein crystallization—is it rocket science? *Drug discovery today*, 6(14), 734-744.
- Dolak, L. A., Castle, T. M., & Laborde, A. L. (1980). 3-Trehalosamine, a new disaccharide antibiotic. *The Journal of antibiotics*, 33(7), 690-694.
- Egan, W. J., Merz, K. M., & Baldwin, J. J. (2000). Prediction of drug absorption using multivariate statistics. *Journal of medicinal chemistry*, 43(21), 3867-3877.
- Egan, W. J., & Lauri, G. (2002). Prediction of intestinal permeability. *Advanced drug delivery reviews*, 54(3), 273-289.
- Fairlamb, I. J., Marrison, L. R., Dickinson, J. M., Lu, F. J., & Schmidt, J. P. (2004). 2-Pyrones possessing antimicrobial and cytotoxic activities. *Bioorganic & medicinal chemistry*, 12(15), 4285-4299.
- Fang, S., Chen, L., Yu, M., Cheng, B., Lin, Y., Morris-Natschke, S. L., ... & Xu, J. (2015). Synthesis, antitumor activity, and mechanism of action of 6-acrylic phenethyl ester-2-pyranone derivatives. *Organic & biomolecular chemistry*, 13(16), 4714-4726.
- Giddens, A. C., Nielsen, L., Boshoff, H. I., Tasdemir, D., Perozzo, R., Kaiser, M., ... & Copp, B. R. (2008). Natural product inhibitors of fatty acid biosynthesis: synthesis of the marine microbial metabolites pseudopyronines A and B and evaluation of their anti-infective activities. *Tetrahedron*, 64(7), 1242-1249.
- Gonzalez, F. J., & Gelboin, H. V. (1992). Human cytochromes P450: evolution and cDNA-directed expression. *Environmental health perspectives*, 98, 81-85.
- Hajduk, P. J., Mack, J. C., Olejniczak, E. T., Park, C., Dandliker, P. J., & Beutel, B. A. (2004). SOS-NMR: a saturation transfer NMR-based method for determining the structures of protein-ligand complexes. *Journal of the American Chemical Society*, 126(8), 2390-2398.
- Hann, M. M., Leach, A. R., & Harper, G. (2001). Molecular complexity and its impact on the probability of finding leads for drug discovery. *Journal of chemical information and computer sciences*, 41(3), 856-864.
- Hoang, V. H., Tran, P. T., Cui, M., Ngo, V. T., Ann, J., Park, J., ... & Ha, H. J. (2017). Discovery of potent human glutaminyl cyclase inhibitors as anti-alzheimer's agents based on rational design. *Journal of medicinal chemistry*, 60(6), 2573-2590.
- Kaloga, M., & Christiansen, I. (1981). Photodimerisierung von 6-trans-Styryl-4-methoxy-2-pyron (= 5,6-Dehydrokawain), 1. Mitteilung/Photodimerisation of 6-trans-Styryl-4-methoxy-2-pyrone (= 5,6-Dehydrokawain). *Zeitschrift für Naturforschung B*, 36(4), 505-507.

23. Kim, Y. S., & Joh, T. H. (2006). Microglia, major player in the brain inflammation: their roles in the pathogenesis of Parkinson's disease. *Experimental & molecular medicine*, 38(4), 333.
24. Kreutzberg, G. W. (1996). Microglia: a sensor for pathological events in the CNS. *Trends in neurosciences*, 19(8), 312-318.
25. Kuntz, I. D., Meng, E. C., & Shoichet, B. K. (1994). Structure-based molecular design. *Accounts of Chemical research*, 27(5), 117-123.
26. Kuroyanagi, M., Yamamoto, Y., Fukushima, S., Ueno, A., Noro, T., & Miyase, T. (1982). Chemical studies on the constituents of *Polygonum nodosum*. *Chemical and Pharmaceutical Bulletin*, 30(5), 1602-1608.
27. Lagorce, D., Reynes, C., Camproux, A. C., Miteva, M. A., Sperandio, O., & Villoutreix, B. O. (2011). In silico adme/tox Predictions. *ADMET for Medicinal Chemists: A Practical Guide*. Hoboken, New Jersey: John Wiley & Sons, Inc, 29-124.
28. Lahti, J. L., Tang, G. W., Capriotti, E., Liu, T., & Altman, R. B. (2012). Bioinformatics and variability in drug response: a protein structural perspective. *Journal of The Royal Society Interface*, 9(72), 1409-1437.
29. Liang, J., Edelsbrunner, H., Fu, P., Sudhakar, P. V., & Subramaniam, S. (1998). Analytical shape computation of macromolecules: I. Molecular area and volume through alpha shape. *Proteins: Structure, Function, and Bioinformatics*, 33(1), 1-17.
30. Lipinski, C. A., Lombardo, F., Dominy, B. W., & Feeney, P. J. (1997). Experimental and computational approaches to estimate solubility and permeability in drug discovery and development settings. *Advanced drug delivery reviews*, 23(1-3), 3-25.
31. Lipinski, C. A. (2016). Rule of five in 2015 and beyond: Target and ligand structural limitations, ligand chemistry structure and drug discovery project decisions. *Advanced drug delivery reviews*, 101, 34-41.
32. Makarov, V., Manina, G., Mikusova, K., Möllmann, U., Ryabova, O., Saint-Joanis, B., ... & Milano, A. (2009). Benzothiazinones kill *Mycobacterium tuberculosis* by blocking arabinan synthesis. *Science*, 324(5928), 801-804.
33. Makarov, V., Lechartier, B., Zhang, M., Neres, J., van der Sar, A. M., Raadsen, S. A., ... & Widmer, N. (2014). Towards a new combination therapy for tuberculosis with next generation benzothiazinones. *EMBO molecular medicine*, 6(3), 372-383.
34. Mascarenhas, Y. P., & Gottlieb, O. R. (1977). Structure of aniba-dimer-a isolated from *Aniba gardneri*. *Phytochemistry*, 16(2), 301-302.
35. Moroy, G., Martiny, V. Y., Vayer, P., Villoutreix, B. O., & Miteva, M. A. (2012). Toward in silico structure-based ADMET prediction in drug discovery. *Drug discovery today*, 17(1-2), 44-55.
36. O'Boyle, N. M., Banck, M., James, C. A., Morley, C., Vandermeersch, T., & Hutchison, G. R. (2011). Open Babel: An open chemical toolbox. *Journal of cheminformatics*, 3(1), 33.
37. Opella, S. J., Ma, C., & Marassi, F. M. (2001). Nuclear magnetic resonance of membrane-associated peptides and proteins. *Methods in enzymology*, 339, 285.
38. Palm, K., Stenberg, P., Luthman, K., & Artursson, P. (1997). Polar molecular surface properties predict the intestinal absorption of drugs in humans. *Pharmaceutical research*, 14(5), 568-571.
39. Parretti, M. F., Kroemer, R. T., Rothman, J. H., & Richards, W. G. (1997). Alignment of molecules by the Monte Carlo optimization of molecular similarity indices. *Journal of computational chemistry*, 18(11), 1344-1353.
40. Peltola, J. S., Andersson, M. A., Kämpfer, P., Auling, G., Kroppenstedt, R. M., Busse, H. J., ... & Rainey, F. A. (2001). Isolation of Toxicogenic *Nocardiosis* Strains from Indoor Environments and Description of Two New *Nocardiosis* Species, *N. exhalans* sp. nov. and *umidiscolae* sp. nov. *Appl. Environ. Microbiol.*, 67(9), 4293-4304.
41. Pliska, V., Testa, B., Van de Waterbeemd, H., Mannhold, R., Kubinyi, H., & Timmerman, H. (Eds.). (1996). *Lipophilicity in drug action and toxicology* (pp. 311-337). Weinheim: VCH.
42. Qing, X., Lee, X. Y., De Raeymaecker, J., Tame, J. R., Zhang, K. Y., De Maeyer, M., & Voet, A. (2014). Pharmacophore modeling: advances, limitations, and current utility in drug discovery. *Journal of Receptor, Ligand and Channel Research*, 7, 81-92.
43. Reymond, J. L., & Awale, M. (2012). Exploring chemical space for drug discovery using the chemical universe database. *ACS chemical neuroscience*, 3(9), 649-657.
44. Sagawa, T., Takaishi, Y., Fujimoto, Y., Duque, C., Osorio, C., Ramos, F., ... & Ahmed, S. U. (2005). Cyclobutane Dimers from the Colombian Medicinal Plant *Achyrocline b ogotensis*. *Journal of natural products*, 68(4), 502-505.
45. Shin, W. H., Christoffer, C. W., Wang, J., & Kihara, D. (2016). PL-PatchSurfer2: improved local surface matching-based virtual screening method that is tolerant to target and ligand structure variation. *Journal of chemical information and modeling*, 56(9), 1676-1691.
46. Stoll, G., Jander, S., & Schroeter, M. (1998). Inflammation and glial responses in ischemic brain lesions. *Progress in neurobiology*, 56(2), 149-171.
47. Tsai, J., Lee, J. T., Wang, W., Zhang, J., Cho, H., Mamo, S., ... & Sproesser, K. (2008). Discovery of a selective inhibitor of oncogenic B-Raf kinase with



- potent antimelanoma activity. *Proceedings of the National Academy of Sciences*, 105(8), 3041-3046.
48. Trott, O., & Olson, A. J. (2010). AutoDock Vina: improving the speed and accuracy of docking with a new scoring function, efficient optimization, and multithreading. *Journal of computational chemistry*, 31(2), 455-461.
49. World Health Organization (WHO). (2016). *World health statistics 2016: monitoring health for the SDGs sustainable development goals*. World Health Organization.
50. Yamashita, T., Imoto, M., Isshiki, K., Sawa, T., Naganawa, H., Kurasawa, S., ... & Umezawa, K. (1988). Isolation of a new indole alkaloid, pendolmycin, from *Nocardioopsis*. *Journal of Natural Products*, 51(6), 1184-1187.
51. Yang, H., Lou, C., Sun, L., Li, J., Cai, Y., Wang, Z., ... & Tang, Y. (2018). admetSAR 2.0: web-service for prediction and optimization of chemical ADMET properties. *Bioinformatics*, 35(6), 1067-1069.
52. Zhao, N., Darby, C. M., Small, J., Bachovchin, D. A., Jiang, X., Burns-Huang, K. E., ... & Cravatt, B. F. (2014). Target-based screen against a periplasmic serine protease that regulates intrabacterial pH homeostasis in *Mycobacterium tuberculosis*. *ACS chemical biology*, 10(2), 364-371.

Received July 14, 2019; revised July 25, 2018; accepted August 15, 2018; published online September 01, 2019